Quantization of false-vacuum bubbles: A Hamiltonian treatment of gravitational tunneling

W. Fischler, D. Morgan, and J. Polchinski
Theory Group, Department of Physics, University of Texas, Austin, Texas 78712
(Received 7 May 1990)

We develop the quantization of spherically symmetric gravitational systems using the Dirac formalism and the WKB approximation. The particular application is the nucleation of false-vacuum bubbles, which may have been the origin of the inflationary universe and matter. Consistency between our results and those obtained by the Euclidean method requires that the latter include metrics with degeneracies. Our work also raises several other questions of principle, including the meaning of the wave function and the necessity of topology change. A tentative application of this work to quantum cosmology indicates that the "Hartle-Hawking wave function" is inconsistent.

I. INTRODUCTION

The vanishing of the cosmological constant is one of the great mysteries in fundamental physics. Because the cosmological constant Λ acts as a source for the gravitational field, many ideas center on some sort of gravitational dynamics. Such ideas have a characteristic problem: since gravity acts universally on all kinds of energy density, a dynamical mechanism which sets Λ to zero also produces an empty universe, without galaxies or life. For example, this is true of the recently proposed Rubakov/googolplexus solution,[1-3] and of several earlier ideas.[4-7]

It has been suggested that the observed universe could have arisen from such an empty or nearly empty state by a gravitational instability, negative gravitational potential energy offsetting the positive energy of matter. One example of such an instability is the false-vacuum bubble.[8-12] A large enough bubble of false vacuum ($\Lambda_F > 0$) embedded in true vacuum ($\Lambda_T = 0$) will grow, the tendency of the false vacuum to inflate overcoming the inward force on the bubble from pressure and tension. This is to be compared with the familiar process of the expansion of a bubble of true vacuum,[13] in which pressure and tension compete. In the case of a bubble of true vacuum, gravitation can either help or hinder the expansion,[14] while in the false-vacuum case it is a necessary ingredient.

The growing-bubble solutions in Refs. 8–12 all originate in singularities, and it has been shown quite generally that a growing false-vacuum bubble cannot develop classically from a nonsingular initial configuration.[15] It might, however, appear as a result of quantum tunneling. The "free lunch" process[16] produces matter in three steps, starting with true vacuum (either empty or possibly containing a small seed for bubble nucleation). In the first step, a false-vacuum bubble large enough to grow appears via quantum tunneling. In the second step this inflates to great size, and in the third a part of the interior decays to true vacuum plus matter energy.

In this paper we investigate the quantum nucleation of the false-vacuum bubble, showing that it can occur and calculating the tunneling amplitude. Because the process involves gravity *and* quantum mechanics in an essential way, it is interesting both technically and conceptually, and leads to a number of results beyond our original motivation. Some of our results have been reported briefly in Ref. 17.

We will analyze the tunneling process using a Hamiltonian approach, rather than the Euclidean path integral. The first reason for this is that the Rubakov/googolplexus idea[1-3] is set in a Hamiltonian framework. The second is that there is a great deal of confusion about the definition and the interpretation of the Euclidean path integral for quantum gravity. Indeed, comparing our results to a recent Euclidean study of the same process by Farhi, Guth, and Guven[18] is very instructive.

In Sec. II we review the canonical Dirac quantization of gravity, and then make the WKB approximation. We assume that the initial and final states, and the path of least action, are spherically symmetric, so we can restrict ourselves to spherically symmetric metrics. There are other gravitational tunneling processes which are spherically symmetric, most notably the wormhole.[19] We expect that our method will also be useful in the interpretation of these. In order to get some practice with the algebra of the WKB approximation, we solve in Sec. III for the wave function of empty Minkoswski space. This system is dynamically trivial, but there are some questions about the interpretation of the wave function whose answers are not clear to us. In Sec. IV we introduce the vacuum bubble in the thin-wall approximation, work out the constraints and matching conditions, and discuss the classical motion. In Sec. V we calculate the WKB nucleation amplitude, both for the false-vacuum bubble of interest here, and as a check, for the true-vacuum bubble studied by Coleman and DeLucchia with the Euclidean formalism.[14] In Sec. VI we compare our approach to other Hamiltonian and Euclidean treatments of this and similar processes.[20-23] In Sec. VII we discuss the implications of our result for topology change and in Sec. VIII we discuss the possibility of getting a free lunch. We also make preliminary application of the spherically symmetric WKB approximation to quantum cosmology. We find that the "Hartle-Hawking wave function," which is a central part of the ideas of Refs. 1–4, appears to suffer from an instability similar to the large-wormhole problem.[24] This may doom yet another class of ideas for the

solution of the cosmological-constant problem. Our conclusions are summarized in Sec. IX. In an appendix we demonstrate that a certain Euclidean spacetime has a degenerate metric, as explained in Sec. VI.

II. CANONICAL QUANTIZATION AND THE WKB APPROXIMATION

We will be studying a bubble with external cosmological constant zero, internal cosmological constant Λ_I, and surface energy per unit area $\mu/4\pi$. For generality, we will consider negative and vanishing Λ_I as well as positive. The bubble will be assumed to be spherical, with a wall of negligible thickness. Since Birkhoff's theorem implies that a spherically symmetric gravitational field has no dynamics, one would expect that the system could be reduced to a single degree of freedom, the bubble radius, with a potential obtained by solving for the gravitational field. However, this approach leads to pathologies, for reasons that we will discuss below and in Sec. V. We will therefore carry out a full-fledged canonical quantization of the spherically symmetric bubble wall and gravitational field.

The general spherically symmetric metric is

$$ds^2=\sum_{\alpha,\beta=t,r} g_{\alpha\beta}(t,r)dx^\alpha dx^\beta + R(t,r)^2(d\theta^2+\sin^2\theta\, d\phi^2) . \tag{1}$$

For the purpose of canonical quantization[25,26] it is useful to write this as

$$ds^2=-N^t(t,r)^2dt^2+L(t,r)^2[dr+N^r(t,r)dt]^2 + R(t,r)^2(d\theta^2+\sin^2\theta\, d\phi^2) , \tag{2}$$

where N^t and N^r are the lapse and shift, L is ds/dr, and R is the transverse radius. The action for gravity plus a general matter theory then takes the form

$$S=\frac{1}{16\pi G}\int d^4x\sqrt{g}\,(\mathbf{R}-2\Lambda)+S_M = \int dt\, p_i\dot{q}^i+\int dr\, dt(\pi_L\dot{L}+\pi_R\dot{R}-N^t\mathcal{H}_t-N^r\mathcal{H}_r) , \tag{3}$$

where M denotes matter, q_i are general matter degrees of freedom, and $\mathcal{H}_t$ and $\mathcal{H}_r$ are the generators of t and r reparametrizations. For the metric (2), the first line of (3) is

$$S=\frac{1}{2G}\int dr\, dt[\,2(N^rLR)'(\dot{R}-N^rR')/N^t -2(LR)^*(\dot{R}-N^rR')/N^t2(N^tR)'R'/L +LN^t+L(\dot{R}-N^rR')^2/N^t -N^tR'^2/L-\Lambda LN^tR^2]+S_M .$$

Since this expression is quadratic in velocities, it can be put in first-order form as in the second line of (3), with

$$\mathcal{H}_t=\frac{GL\pi_L^2}{2R^2}-\frac{G\pi_L\pi_R}{R} +\frac{1}{2G}\left[\left[\frac{2RR'}{L}\right]'-\frac{R'^2}{L}-L+\Lambda LR^2\right]+\mathcal{H}_{tM} , \qquad \mathcal{H}_r=R'\pi_R-L\pi_L'+\mathcal{H}_{rM} . \tag{4}$$

A prime denotes d/dr. The momenta and velocities are related by

$$\pi_R=\frac{1}{2G}[2(N^rLR)'/N^t-2(LR)^*/N^t] , \qquad \pi_L=\frac{1}{2G}[-2R(\dot{R}-N^rR')/N^t]$$

and

$$\dot{R}=-GN^t\pi_LR^{-1}+N^rR' , \qquad \dot{L}=-GN^t\pi_RR^{-1}+GLN^t\pi_LR^{-2}+(N^rL)' .$$

The time derivatives of the lapse and shift do not appear in the action, so there are primary constraints

$$\pi_{N^t}(r)=\pi_{N^r}(r)=0 . \tag{5}$$

These have nonvanishing Poisson brackets with the Hamiltonian, leading to vanishing of the Hamiltonian and momentum densities as secondary constraints:

$$\mathcal{H}_{t,r}(r;\pi_L,\pi_R,p,L,R,q)=0 . \tag{6}$$

In Dirac's canonical quantization[25] the constraints are imposed on the state,

$$\pi_{N^t,N^r}(r)\Psi=\mathcal{H}_{t,r}(r)\Psi=0 . \tag{7}$$

The constraints are first class: classically, their Poisson brackets close with no central charge. Equations (7) are therefore consistent in the leading WKB approximation. At higher orders, there would be the possibility of Schwinger terms in the algebra, and it is necessary to carry out a more sophisticated quantization such as that of Becchi, Rouet, Stora, and Tyutin.[27]

By the primary constraints, $\Psi(N^t,N^r,L,R,q)$ is independent of N^t and N^r, so that it depends only on the spatial geometry and the matter configuration:

$$\Psi(L,R,q) . \tag{8}$$

The $\mathcal{H}_r$ constraint is also simple, requiring amplitudes to be equal for two configurations which differ only by a reparametrization $r'(r)$. The $\mathcal{H}_t$ constraint is more complicated, "dynamical," because it is second order in momenta.

Note that we are distinguishing Dirac quantization from Arnowitt-Deser-Misner (ADM) quantization.[26] The Dirac wave function (8) involves no fixing of gauge: it gives the amplitude for *all* possible time slices and radial parametrizations. In the ADM quantization, the slicing and parametrization are fixed by a gauge choice. For the radial parametrization a simple gauge choice is $L(r)=1$, so that the radial coordinate measures proper distance. For the time slicing, ADM make various choices, such as the minimal gauge

$$\pi_i^i=L\pi_L+2R\pi_R=0 . \tag{9}$$

By making such gauge choices, ADM reduce the system to its "true" dynamical degrees of freedom. In the case of the bubble wall, this would leave just the one degree of freedom expected.

However, the gauge choice must be a "good" one. There is a difference here between t and r, because of the dynamical nature of $\mathcal{H}_t$. For the radial parametrization,

it is clear that the choice $L(r)=1$ precisely fixes the coordinate freedom. It is not hard to find a good time slicing also, if one is perturbing around a given background as were ADM. But for our tunneling problem, where the gravitational field is making a large excursion, it is not clear how to distinguish a good time slicing from a bad one *a priori*. As we show in Sec. V, it turns out that some of the simplest choices are bad. Therefore we will work with the full-fledged Dirac formalism.

In the WKB approximation, expand

$$\Psi(L,R,q)=\exp[i\Sigma_0(L,R,q)/\hbar+O(\hbar^0)] . \tag{10}$$

To leading order in $\hbar$, the secondary constraints become Hamilton-Jacobi equations,

$$\mathcal{H}_{t,r}\left[r;\frac{\delta\Sigma_0}{\delta L},\frac{\delta\Sigma_0}{\delta R},\frac{\delta\Sigma_0}{\delta q},L,R,q\right]=0 . \tag{11}$$

In one-dimensional quantum mechanics, the WKB equation determines the derivative $\delta\Sigma_0/\delta q$ (up to the usual sign choice) as a function of q and the energy E. As we have noted, the gravitating bubble should, by Birkhoff's theorem, have essentially the same number of dynamical degrees of freedom as one-dimensional quantum mechanics. Correspondingly, we will find in Sec. V that the Hamilton-Jacobi equations (11) determine, up to sign, all derivatives of Σ_0 with respect to the configuration $L(r),R(r),\hat{r}$ ($\hat{r}$ is the coordinate radius of the bubble), as a function of the configuration and of the asymptotic Schwarzschild mass of the system, M. Again, the equations are consistent because the algebra of constraints is first class.

Quantum gravity restricted to spherically symmetric fields is a version of minisuperspace known as the Berger-Chitre-Moncrief-Nutku (BCMN) model.[28–30] We should point out that, as long as we are interested only in the leading WKB approximation, we obtain the same result whether we restrict to spherical symmetry before or after quantization. In the latter case there are additional constraints from angular reparametrizations, and additional terms in the t,r constraints, but these all vanish for spherical symmetry. At the next order in the WKB approximation, we would have to consider nonspherically symmetric fluctuations (as well as the central charges mentioned above). However, Hamiltonian methods are clumsy in any case for higher order WKB calculations in field theory—the path integral formalism is vastly simpler, if it can be developed. We are using the Hamiltonian formalism for conceptual, not calculational, reasons.

III. EMPTY MINKOWSKI SPACE

We now wish to study the solution of the Hamilton-Jacobi equations (11). It is useful to eliminate π_R by forming the combination

$$0=\frac{R'}{L}\mathcal{H}_t+\frac{G\pi_L}{RL}\mathcal{H}_r=-\mathcal{M}'+\frac{R'}{L}\mathcal{H}_{tM}+\frac{G\pi_L}{RL}\mathcal{H}_{rM} , \tag{12}$$

where

$$\mathcal{M}=\frac{G\pi_L^2}{2R}+\frac{R}{2G}\left[1-\left[\frac{R'}{L}\right]^2-\frac{\Lambda R^2}{3}\right] . \tag{13}$$

The quantity $\mathcal{M}$ has a simple interpretation. By considering a static slice ($\pi_{L,R}=0$) in the absence of matter (so that $\mathcal{M}'=0$), Eq. (13) becomes the differential equation which describes a static slice in Schwarzschild or Schwarzschild-de Sitter spacetime, with $\mathcal{M}$ the mass parameter. The constraint (12) is thus a gravitational analog of Gauss's law.

For practice, we first study empty Minkowski spacetime, with $\Lambda=0$. The radial coordinate runs from 0 to ∞, with $R(0)=0$. The condition that the origin be nonsingular determines $\mathcal{M}(0)=0$. The constraint (12) then implies that $\mathcal{M}(r)=0$, and so

$$\pi_L^2=\frac{R^2}{G^2}[(R'/L)^2-1] . \tag{14}$$

From this we see that the classically allowed and forbidden regions are

$$\begin{aligned}&\text{Allowed:}\quad |R'(r)|\geq L(r) ,\\ &\text{Forbidden:}\quad |R'(r)|<L(r) .\end{aligned} \tag{15}$$

Notice that a given spatial geometry can be classically allowed in some regions and forbidden in others. For our purposes it will always be sufficient to consider 3-geometries which are either allowed everywhere or forbidden everywhere. In the present case, the allowed and forbidden 3-geometries have a simple interpretation: the allowed 3-geometries are precisely those which can be obtained by some time slice through classical Minkowski space.

In the allowed region, solve Eq. (14) for π_L and then use the $\mathcal{H}_r$ constraint $\pi_R=L\pi_L'/R'$ to obtain

$$\begin{aligned}\pi_L&=\eta\frac{R}{GL}\sqrt{R'^2-L^2} ,\\ \pi_R&=\eta\frac{R'^2+RR''-R'L'/L-L^2}{G\sqrt{R'^2-L^2}} ,\end{aligned} \tag{16}$$

where $\eta=\pm1$.[31]

Now integrate the Hamilton-Jacobi equation,

$$\delta\Sigma_0=\int_0^\infty dr\,[\delta L(r)\pi_L(r)+\delta R(r)\pi_R(r)] . \tag{17}$$

An easy way to do this is first to integrate with respect to $L(r)$, along a path of constant $R(r)$, to $L(r)=R'(r)$ (the boundary between allowed and forbidden 3-geometries). Then, holding $L(r)=R'(r)$, integrate to a standard configuration like $L(r)=1,R(r)=r$. The second leg makes no contribution, because the momenta vanish. This gives

$$\Sigma_0^{A\eta}=\frac{\eta}{G}\int_0^\infty dr\,[R\sqrt{R'^2-L^2}-RR'\operatorname{arccosh}(R'/L)] , \tag{18}$$

where the arccosh is defined to be positive.

In the forbidden region, the momenta are

$$i\pi_L=\eta'\frac{R}{GL}\sqrt{L^2-R'^2} , \tag{19}$$

$$i\pi_R = -\eta' \frac{R'^2 + RR'' - R'L'/L - L^2}{G\sqrt{L^2 - R'^2}} .$$

The integral of Eq. (17) is

$$i\Sigma_0^{F\eta'} = \frac{\eta'}{G} \int_0^\infty dr [R\sqrt{L^2 - R'^2} - RR' \arccos(R'/L)] , \tag{20}$$

where $0 \le \arccos \le \pi$. As usual, the decreasing wave function

$$\Psi^{F-} \sim e^{i\Sigma_0^{F-}} \tag{21}$$

connects to a linear combination of the two allowed wave functions. As already noted, the determination of the prefactor, the next WKB correction, is a difficult task which we will not attempt.

The calculation which we have just done is only a warmup; we would like to pause and raise a few questions about the result. In particular, does the wave function that we have calculated mean anything? One is tempted to say no, because this system has no dynamical degrees of freedom. In the ADM approach, this would be made explicit by a gauge choice, such as $L(r)=1, \pi_L(r)=0$. On the other hand, once a measuring apparatus is added, the combined system does have dynamics—the question, whose answer we do not know, is whether it is possible to devise an apparatus whose own quantum fluctuations and gravitational effect are small enough to allow the wave function of the empty vacuum to be observed.

In this same vein, there is a simple example which shows that the wave function, for gauge degrees of freedom, should not be taken too seriously. This is the wave function of the string, in Minkowski spacetime. For example, the tachyon wave function is

$$\Psi(X) = e^{ik\cdot X_0} e^{-(1/2)\int\int X'^\mu(\sigma)|\partial_\sigma^{-1}|X'_\mu(\sigma')} , \tag{22}$$

where $X^\mu(\sigma) = X_0^\mu + X'^\mu(\sigma)$. Lorentz invariance forces the wave function for X'^0 to be a wrong-sign Gaussian. Thus we clearly cannot interpret Eq. (22) literally as a probability amplitude. As has been discussed many times, there is a very close analogy between the embedding time in string theory and the scale of the metric in general relativity. So it is not even clear that the decaying exponential (21) is the correct choice for the Minkowski vacuum.[32]

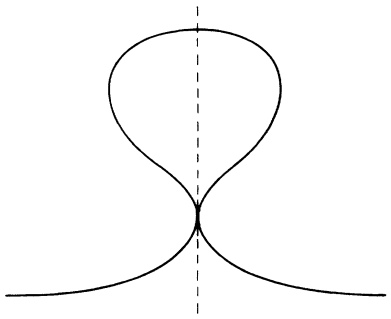

FIG. 1. A spatial geometry on the boundary of configuration space. Figures 1, 2, 4, and 5 show fixed θ, ϕ slices through various spatial geometries. In each figure, the transverse radius R is given by the orthogonal distance from the vertical axis, while radial proper distance $L\,dr$ is measured along the curve.

We would like to raise one final conjecture. This concerns the question, does topology change occur in quantum gravity? In particular, is there some argument which shows that the consistency of the theory either requires it, or forbids it? Consider a 3-geometry like that shown in Fig. 1, in which $R(r)$ doubles back to zero: it is on the boundary of configuration space. This is in the forbidden region, but the wave function for this 3-geometry does not vanish. Thus, there is the possibility of probability flowing out through the boundary. We conjecture that it is not possible to make the Hamiltonian density self-adjoint entirely within the one-universe sector, but that we need to adjoin a two-universe sector in which the teardrop in Fig. 1 has broken off entirely, and so on. This is similar to the original derivation of the Rubakov-Callan effect, monopole catalysis of baryon number violation.[33] In that case, even without knowledge of the short-distance theory (the monopole core), conservation of probability guarantees that catalysis must occur.

IV. THE FALSE-VACUUM BUBBLE

We now extend the previous discussion to include the vacuum bubble, whose parameters were described at the beginning of Sec. II. We work out the constraints and matching conditions, and review the relevant results about the classical motion of the bubble.

The action for the bubble plus gravity is

$$\begin{aligned} S &= \frac{1}{16\pi G} \int d^4x \sqrt{g}\, \mathbf{R} - \frac{\Lambda_I}{8\pi G} \int_{\text{interior}} d^4x \sqrt{g} \\ &\quad - \frac{\mu}{4\pi} \int_{\text{wall}} d^3A \\ &= \frac{1}{16\pi G} \int d^4x \sqrt{g}\, \mathbf{R} - \frac{\Lambda_I}{2G} \int dt \int_0^{\hat r} dr\, N^t L R^2 \\ &\quad - \mu \int dt\, \hat R^2 [\hat N^{t2} - \hat L^2 (\dot{\hat r} + \hat N^r)^2]^{1/2} , \end{aligned} \tag{23}$$

where $\hat r$ is the coordinate radius of the bubble and a caret on a function (such as R) indicates that it is to be evaluated at $\hat r, \hat R = R(\hat r)$. From this we derive the Hamiltonian and momentum densities

$$\begin{aligned} \mathcal{H}_t(r) &= \frac{GL\pi_L^2}{2R^2} - \frac{G\pi_L\pi_R}{R} + \frac{1}{2G}\left[\left[\frac{2RR'}{L}\right]' - \frac{R'^2}{L} - L\right] \\ &\quad + \theta(\hat r - r)\frac{\Lambda_I}{2G} LR^2 + \delta(\hat r - r)(L^{-2}\hat p^2 + \mu^2 \hat R^4)^{1/2} , \\ \mathcal{H}_r(r) &= R'\pi_R - L\pi'_L - \delta(\hat r - r)\hat p , \end{aligned} \tag{24}$$

where $\hat p$ is the momentum conjugate to $\hat r$, and $\hat E = (\hat p^2 + \mu^2 L^2 \hat R^4)^{1/2}$.

In the interior of the bubble, $\mathcal{M}(r)$ defined by Eq. (13) with cosmological constant Λ_I is r independent, while in the exterior $\mathcal{M}(r)$ with zero cosmological constant is r independent. The condition that the origin be nonsingular fixes $\mathcal{M}(0)=0$. If we study a system of definite mass M, we also have the boundary condition $\mathcal{M}(\infty)=M$. Now knowing $\mathcal{M}(r)$, we can solve Eq. (13) for the momenta:

$$r<\hat{r},\quad \pi_L^2=\frac{R^2}{G^2}\left[\frac{R'^2}{L^2}-1+\frac{\Lambda_I R^2}{3}\right];$$
$$r>\hat{r},\quad \pi_L^2=\frac{R^2}{G^2}\left[\frac{R'^2}{L^2}-1+\frac{2GM}{R}\right]. \tag{25}$$

The vanishing of the densities (24) also provides matching conditions at the bubble wall. We will take the geometry at the wall to be as smooth as possible. The constraints are consistent with the spatial geometry $L(r),R(r)$ being continuous at $\hat{r}$ and the momenta $\pi_L(r),\pi_R(r)$ being free of δ functions there. With these assumptions the constraints imply the following discontinuities at the wall:

$$\Delta\pi_L=-\frac{\hat{P}}{\hat{L}},$$
$$\Delta R'=-\frac{G\hat{E}}{\hat{R}}. \tag{26}$$

It is also useful to write the results (25) and the matching conditions (26) in terms of the two-component vectors

$$\mathbf{V}(r)=\left[\frac{R'(r)}{L(r)},\frac{G\pi_L(r)}{R(r)}\right],$$
$$\mathbf{V}_M=\left[\frac{G\hat{E}}{\hat{R}},\frac{G\hat{p}}{\hat{R}}\right]. \tag{27}$$

The solution (25) to the constraints now takes the form

$$r<\hat{r},\quad \mathbf{V}\cdot\mathbf{V}(r)=1-\frac{\Lambda_I R^2(r)}{3};$$
$$r>\hat{r},\quad \mathbf{V}\cdot\mathbf{V}(r)=1-\frac{2GM}{R(r)}, \tag{28}$$

with the Lorentzian dot product

$$\mathbf{V}\cdot\mathbf{V}'=V_1V_1'-V_2V_2'. \tag{29}$$

Also, by definition,

$$\mathbf{V}_M\cdot\mathbf{V}_M=\mu^2\hat{L}^2\hat{R}^4. \tag{30}$$

The matching conditions (26) are simply

$$\mathbf{V}(\hat{r}+\epsilon)-\mathbf{V}(\hat{r}-\epsilon)=-\mathbf{V}_M. \tag{31}$$

Equations (28), (30), and (31) have an obvious SO(1,1) symmetry, arising from the coordinate invariance. They give five conditions on the six components of $\mathbf{V}(\hat{r}+\epsilon)$, $\mathbf{V}(\hat{r}-\epsilon)$, and $\mathbf{V}_M$, fixing these vectors up to an SO(1,1) rotation. It is convenient to make such a rotation so as to set $\hat{p}=0$, corresponding to the rest frame of the wall. In this frame, one can solve for the remaining components, giving

$$R'(\hat{r}-\epsilon)=\frac{M\hat{L}}{\mu\hat{R}^2}-\frac{G\hat{L}\hat{R}\mu}{2}(\lambda-1),$$
$$R'(\hat{r}+\epsilon)=\frac{M\hat{L}}{\mu\hat{R}^2}-\frac{G\hat{L}\hat{R}\mu}{2}(\lambda+1), \tag{32}$$
$$\pi_L^2(\hat{r}-\epsilon)=\pi_L^2(\hat{r}+\epsilon)$$
$$=\frac{\mu^2\hat{R}^4}{4}[(2\rho-1-\lambda)^2+8\rho-4(\rho/G^2\mu M)^{2/3}],$$

where

$$\lambda=\frac{\Lambda_I}{3G^2\mu^2},\quad \rho=\frac{M}{G\mu^2\hat{R}^3}. \tag{33}$$

From the result (32), one can derive certain key features of the classical motion. These classical motions have been extensively studied in Refs. 8–12; we will use the notation and terminology of Ref. 12. First, π_L^2 is always positive as $\hat{R}\to 0$ and $\hat{R}\to\infty$, corresponding to classically allowed motion. Now vary M, holding fixed the other parameters μ and Λ_I. One can see that for M sufficiently large, $M>M_{\rm cr}$, π_L^2 is positive for all $\hat{R}$: there are no turning points. The classical bubble emerges from an initial Schwarzschild singularity and inflates indefinitely (or the time reversed process). This is the type E trajectory.[12] For $M<M_{\rm cr}$, there is a range $R_1<\hat{R}<R_2$ in which π_L^2 is negative and classical motion is forbidden. The turning radii always satisfy

$$R_S<R_1<R_2<R_D, \tag{34}$$

where R_S is the Schwarzschild radius $2GM$, and R_D is the de Sitter radius $\sqrt{3/\Lambda_I}$. For $\hat{R}\le R_1$ there is a classical solution in which the bubble emerges from a Schwarzschild singularity, expands to R_1, and then collapses to a Schwarzschild singularity, the type A/B trajectory. For $\hat{R}\ge R_2$ there is a solution in which the bubble contracts from infinite radius to R_2 and then reinflates, the type C/D trajectory.[34]

At the turning point 3-geometries, all momenta vanish,

$$\pi_L(r)=\pi_R(r)=\hat{p}=0. \tag{35}$$

Equation (25) can then be integrated to determine $R(r)$: the interior of the bubble is a static slice of de Sitter space, and the exterior is a static slice of Schwarzschild space. The signs of $R'(\hat{r}-\epsilon)$ and $R'(\hat{r}+\epsilon)$ in the turning point 3-geometries are significant. If $R'(\hat{r}+\epsilon)$ is positive, $R(r)$ increases monotonically in the exterior. If it is negative, then $R(r)$ decreases to R_S before increasing to infinity: this is a Schwarzschild wormhole, or Einstein-Rosen bridge. If $R'(\hat{r}-\epsilon)$ is positive, the interior is less than half of a three-sphere; if it is negative, the interior is more than half of a three-sphere. We now quote the following results,[12] which can also be deduced from Eq. (32). There are two masses M_S and M_D at which the character of the turning point changes, and these are ordered

$$M_D<M_S<M_{\rm cr}. \tag{36}$$

For the inner turning 3-geometry, $R'(\hat{r}-\epsilon)$ is always positive, while $R'(\hat{r}+\epsilon)$ is positive for $M<M_S$ (type A) and negative for $M>M_S$ (type B). For the outer turning 3-geometry, $R'(\hat{r}-\epsilon)$ is positive for $M>M_D$ (type D) and negative for $M<M_D$ (type C), while $R'(\hat{r}+\epsilon)$ is always negative: there is a Schwarzschild wormhole.

V. QUANTUM NUCLEATION

Spacetimes C, D, and E, with inflating false-vacuum bubbles, have past singularities. In Ref. 15, this was shown to be a general result: any classical spacetime with such a bubble must have a past singularity. On the other hand, the type A subcritical bubble may have a nonsingu-

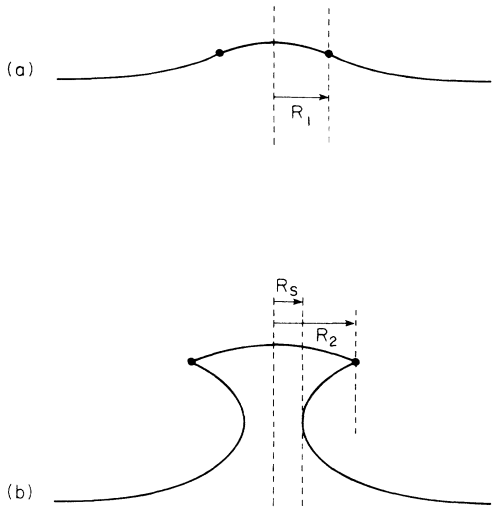

FIG. 2. Two turning geometries. (a) The subcritical seed geometry. (b) The critical bubble, which subsequently expands.

lar past. Although in the present case the type A trajectory emerges from a singularity, there are various ways to avoid this: endowing the bubble with global or gauge charges so that it becomes a nontopological soliton, or arranging that the thin-wall approximation breaks down at $\hat{R} \gg R_S$. In the latter case, the analog of trajectory type A would describe the bubble forming from, and then breaking apart into, ordinary quanta.

The process in which we are interested is the tunneling of the "buildable" type A bubble from the inner turning point R_1, through the forbidden region, to the outer turning point R_2, from which it evolves classically on the type C or D trajectory. This would be a quantum violation of the classical no-go theorem, and would initiate the free lunch process. The two turning-point 3-geometries are shown in Fig. 2. In Fig. 3 we show the Schwarzschild geometry outside the bubble as a static slice on the Kruskal diagram. The bubble wall starts in ordinary spacetime, region I, and appears to tunnel through the Schwarzschild wormhole to region III. (Actually, for reasons to be explained in the next section, we do not think about the tunneling in quite this way.) Classically, region III is causally disconnected from region I, so this is a quantum violation of the usual causal structure.

We will calculate the WKB wave function for the bubble plus gravity, and identify the ratio of the wave function at the inner and outer turning points as the first approximation to the tunneling amplitude.[35] The ratio is obtained by integrating the Hamilton-Jacobi equation along any smooth path connecting the initial and final 3-geometries. In order to verify that there is no subtle barrier to the tunneling process, we will first construct explicitly one such path; however, the calculation of the amplitude will not depend on the details of the path. We will choose the path so that

$$L(r)=1 \tag{37}$$

and

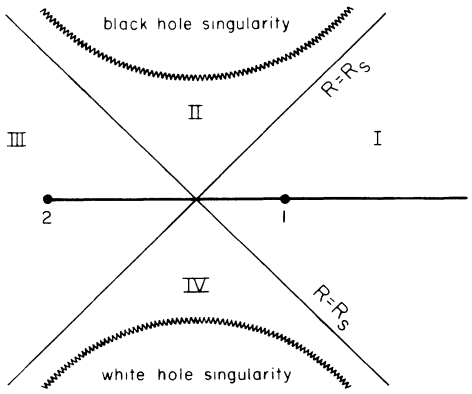

FIG. 3. A Kruskal diagram of Schwarzschild spacetime, with a static slice indicated by the bold line. The exterior of the subcritical seed bubble corresponds to right of the point 1 on the slice. The exterior of the critical bubble corresponds to the right of point 2. The bubble expands in region III.

$$\begin{aligned} r<\hat{r}:\ & i\pi_L(r)=K(\hat{R})\left[\frac{R(r)}{\hat{R}}\right]^a , \\ r>\hat{r}:\ & i\pi_L(r)=K(\hat{R})\left[\frac{R(r)}{\hat{R}}\right]^{-b} . \end{aligned} \tag{38}$$

Here, a and b are any constants greater than 1, and

$$K(\hat{R})=\eta'\frac{\mu\hat{R}^2}{2}[\,4(\rho/G^2\mu M)^{2/3} -(2\rho-1-\lambda)^2-8\rho]^{1/2} . \tag{39}$$

This is consistent with the solution (32) of the matching conditions, and the argument of the square root is positive in the forbidden region.

To see that the condition (38) fixes the 3-geometry, combine it with the solution (25) to the constraints, giving

$$\begin{aligned} r<\hat{r}:\ & R'^2+V_I(R;\hat{R})=0 , \\ r>\hat{r}:\ & R'^2+V_O(R;\hat{R})=0 , \end{aligned} \tag{40}$$

where

$$\begin{aligned} V_I(R;\hat{R})&=-1+\frac{\Lambda}{3}R^2+\frac{G^2K^2(\hat{R}^2)}{4\hat{R}^{2a}}R^{2a-2} , \\ V_O(R;\hat{R})&=-1+\frac{2GM}{R}+\frac{G^2K^2(\hat{R}^2)}{4\hat{R}^{-2b}}R^{-2b-2} . \end{aligned} \tag{41}$$

These can be thought of as representing conservation of energy for a particle moving in a potential, the potential changing at "time" $r=\hat{r}$. The radius $\hat{R}$ of the wall appears as a parameter in the potential. The boundary conditions

$$R(0)=0, \quad R'(0)=1 , \tag{42}$$

together with the jump condition $\Delta R'=-G\mu\hat{R}$ following from the matching condition (26), completely determine the motion of the particle—that is, the 3-geometry. Further, the equation, and its solution, depend in a smooth way on the radius $\hat{R}$. When $\hat{R}=R_{1,2}$, $K(\hat{R})$ vanishes

and the 3-geometry just defined reduces to the turning-point 3-geometry. Pictorially one can imagine interpolating between Figs. 2(a) and 2(b) by expanding the radius $\hat{R}$ while pinching in the outer geometry to form the Schwarzschild wormhole.

The Hamilton-Jacobi equation is now

$$\delta\Sigma_0=\delta\hat{r}\hat{p}\int_0^\infty dr[\delta L(r)\pi_L(r)+\delta_R(r)\pi_R(r)]\ . \tag{43}$$

To integrate, first hold fixed $\hat{r}$ and the geometry in a neighborhood of the wall, while varying L and R elsewhere. With the momenta given by Eq. (25), this gives

$$i\Sigma_0^{F\eta'}=\eta'(F_I+\hat{F}+F_O)\ , \tag{44}$$

where

$$F_I=\frac{1}{G}\int_0^{\hat{r}}dr[\,R\sqrt{L^2-\Lambda_I L^2R^2/3-R'^2}\,-RR'\arccos(R'/L\sqrt{1-\Lambda_I R^2/3})]\ , \tag{45}$$

$$F_O=\frac{1}{G}\int_{\hat{r}}^\infty dr[\,R\sqrt{L^2-2GML^2/R-R'^2}\,-RR'\arccos(R'/L\sqrt{1-2GM/R}\,)]\ ,$$

and where $\hat{F}$ depends only on the geometry at the wall. The forms of F_I and F_O are determined in the same way as the similar results (18) and (20) for empty Minkowski space. Again, the inverse cosine is defined to lie between 0 and π. To obtain $\hat{F}$, allow a variation of $L(r)$ and $R(r)$ which is nontrivial at the wall, with the result

$$\delta\hat{F}=\delta\hat{R}\frac{\hat{R}}{G}\{\arccos[R'(\hat{r}-\epsilon)/\hat{L}\sqrt{1-\Lambda_I\hat{R}^2/3}]-\arccos[R'(\hat{r}+\epsilon)/\hat{L}\sqrt{1-2GM/\hat{R}}\,]\}\ . \tag{46}$$

The right-hand side comes from a total derivative in relating $\delta F_{I,O}/\delta R$ to $\int\delta R\,\pi_R$. In Eq. (46), $\delta\hat{F}$ depends on the geometry only through the value of $\hat{R}$. In particular, $R'(\hat{r}\pm\epsilon)/L$ was determined in terms of $\hat{R}$ in the solution (32) to the matching conditions. Thus, $\hat{F}$ is obtained by integrating Eq. (46) with respect to $\hat{R}$. We have not considered variations of $\hat{r}$, but the integrability of the equations ensures that this will be correct, and one can check it explicitly.

In all,

$$\ln\Psi^{F\eta'}[R_2-R_1]=\frac{\eta'}{\hbar}(F_I[R_2-R_1]+F_O[R_2-R_1]+\hat{F}[R_2-R_1])\ , \tag{47}$$

where $[R_2-R_1]$ means the difference in the quantity evaluated at the two turning-point geometries. The integrals $F_{I,O}$ simplify greatly at the turning points. The first term vanishes, and the arccos is 0 if $R'>0$ and π if $R'<0$. Thus, $F_{I,O}$ get contributions only where the geometry "back tracks":

$$F_I[R_2-R_1]+F_O[R_2-R_1]=\begin{cases}\frac{\pi}{2G}(R_2^2-R_1^2), & M>M_S\ ,\\ \frac{\pi}{2G}(R_2^2-R_S^2), & M_S>M>M_D\ ,\\ \frac{\pi}{2G}(R_D^2-R_S^2), & M_D>M\ .\end{cases} \tag{48}$$

Also,

$$\hat{F}[R_2-R_1]=\frac{1}{G}\int_{R_1}^{R_2}d\hat{R}\left[\hat{R}\arccos\left[\frac{2M-G\mu^2\hat{R}^3(\lambda-1)}{2\mu\hat{R}^2\sqrt{1-\Lambda_I R^2/3}}\right]-\hat{R}\arccos\left[\frac{2M-G\mu^2\hat{R}^3(\lambda+1)}{2\mu\hat{R}^2\sqrt{1-2GM/R}}\right]\right]\ . \tag{49}$$

The right-hand side of Eq. (47) is negative for $\eta'=-1$. The tunneling probability is

$$P\sim e^{-2(F_I[R_2-R_1]+F_O[R_2-R_1]+\hat{F}[R_2-R_1])/\hbar}\ . \tag{50}$$

Let us relate this result to our earlier work.[17] There we made a different choice of interpolating geometries, namely the minimal gauge. In particular, this fixed $\pi_{L,R}=0$ inside the wall. Unlike the choice (38) described above, the geometry defined by the minimal gauge is *not* a continuous function of $\hat{R}$ for all values of the parameters—it only works for M greater than some mass $\tilde{M}$, where $M_S>\tilde{M}>M_D$. In Ref. 17, only the range $M_S>M>\tilde{M}$ was considered. The present choice of interpolating geometries works for arbitrary values of the parameters.

The forms given for $\hat{F}$, Eq. (10) of Ref. 17 and Eqs. (46) and (49) above, differ, but it is easily seen that they are equivalent. The inverse cosines in Eq. (46) are just the angles $\theta^{\mp}$ defined by the vectors $\mathbf{V}(\hat{r}-\epsilon)$ and $\mathbf{V}(\hat{r}+\epsilon)$ (in the Euclidean plane, because we are in the forbidden region). The minimal gauge and the gauge (38) differ by an SO(2) rotation at the wall. Both expressions for $\hat{F}$ involve $\theta^--\theta^+$ which is an SO(2) invariant. With the minimal slicing, θ^- vanishes.

It is interesting also to consider the case $\Lambda_I<0$, so that the exterior, $\Lambda=0$, is false vacuum. We take $M=0$, corresponding to the spontaneous decay of the false vacuum, which was studied by Coleman and DeLucchia[14] using the Euclidean bounce method. Then the solution (32) to

the matching conditions becomes

$$R'(\hat{r}-\epsilon)=\frac{G\hat{L}\hat{R}\mu}{2}(|\lambda|+1)\ ,$$
$$R'(\hat{r}+\epsilon)=\frac{G\hat{L}\hat{R}\mu}{2}(|\lambda|-1)\ , \tag{51}$$
$$\pi_L^2(\hat{r}-\epsilon)=\pi_L^2(\hat{r}+\epsilon)=\frac{\mu^2\hat{R}^2}{4}(|\lambda|-1)^2-1/4G^2\ .$$

The region $\hat{R}<R_C$ is forbidden, and $\hat{R}>R_C$ is allowed, where $R_C=1/G\mu(|\lambda|-1)$. Notice that the critical radius diverges when $|\lambda|=1$. For $|\lambda|<1$ the tunneling is actually impossible:[14] the turning geometry is not a bubble of true vacuum in false, but a compact space, half true vacuum and half false.

The tunneling amplitude is now obtained immediately from the results (45) and (46). In this case, F_I and F_O vanish at both turning points, and

$$\begin{aligned}\hat{F}[R_C-0]&=\int_0^{R_C}d\hat{R}\left[\arccos\frac{G\hat{R}\mu(|\lambda|+1)}{2\sqrt{1+|\Lambda|\hat{R}^2/3}}-\arccos\frac{G\hat{R}\mu(|\lambda|-1)}{2}\right]\\&=\int_0^{(|\lambda|-1)^{-1}}dx\ \arccos\frac{2+x^2(|\lambda|-1)}{2\sqrt{1+|\lambda|x^2}}\\&=-\frac{\pi}{2G^3\mu^2|\lambda|(|\lambda|-1)^2}\ .\end{aligned} \tag{52}$$

The tunneling amplitude,

$$\frac{\Psi^{F+}[R_C]}{\Psi^{F+}[0]}=e^{2\hat{F}[R_c-0]}\ , \tag{53}$$

agrees with Coleman and DeLucchia.[14,36]

VI. COMPARISON WITH OTHER WORK

We have studied the false-vacuum bubble using Dirac quantization. As we have noted, there are two natural alternatives: reduction to a single quantum mechanical degree of freedom, as in the ADM method, and the Euclidean bounce method. We consider the former first.

The Dirac quantization, describing simultaneously all possible ways of choosing space-time coordinates, contains a large amount of redundant information. We could reduce this to the expected single degree of freedom by gauge fixing, choosing a family of spatial configurations parametrized by a single variable y,

$$\hat{r}(y),\quad L(r;y),\quad R(r;y)\ . \tag{54}$$

The momentum conjugate to y is given by the chain rule,

$$p_y=\frac{\partial\hat{r}}{\partial y}\hat{p}+\int_0^\infty dy\frac{\partial L(r)}{\partial y}\pi_L(r)+\frac{\partial R(r)}{\partial y}\pi_R(r)\ . \tag{55}$$

The constraints give just enough information to solve for p_y in terms of y and the Schwarzschild mass M. Inverting gives the Schwarzschild mass

$$M(y,p_y)\ , \tag{56}$$

which, up to the usual ordering problems, is the global Hamiltonian for the system.

A seemingly natural choice of slice is to take the geometry to be static de Sitter inside and static Minkowski outside, with the wall radius $\hat{R}$ being the dynamical variable y. This is the choice made by Berezin, Kozimirov, Kuzmin, and Tkachev,[20] and in the Hamiltonian treatment of Farhi, Guth, and Guven.[18,37] There are, however, some problems with this choice. First, it is impossible when $\hat{R}<R_S$ or $\hat{R}>R_D$. Second, in the range $R_S<\hat{R}<R_D$ there are four branches, depending on whether the spatial geometry includes more or less than half of the de Sitter sphere, and more or less than half of the vacuum Schwarzschild space. The process that we are interested in, tunneling from a type A trajectory to type C or D, involves tunneling from one branch to another, and it is not clear how this can be addressed in this gauge. Reference 18 discusses extensively the pathologies of the Hamiltonian obtained in this slicing.

An alternative choice of gauge is the one that we have used in the preceding section, Eq. (38). This assigns a unique spatial geometry to each radius $\hat{R}$, and the Hamiltonian has the expected character, allowed regions $\hat{R}<R_1$ and $\hat{R}>R_2$ separated by a forbidden region. By construction, the tunneling amplitude in this reduced quantum mechanical system is identical to that which we have obtained. However, our description of the slicing has necessarily been somewhat implicit, and so we are unable to give the Hamiltonian in closed form. Notice that the radius $\hat{R}$ increases monotonically from R_1 to R_2 on our path, and never drops to the Schwarzschild value R_S. The wall thus does not tunnel through the Schwarzschild wormhole; rather, space bulges inward around it to form the wormhole. Both the wall *and* the geometry tunnel.

It is not clear how to distinguish a good gauge from a bad one *a priori*, and so we have avoided this by working in the gauge-invariant Dirac formalism. However, we would like to make a few remarks. When fixing gauge in the Lagrangian formalism, the definition of a good gauge is straightforward: it intersects each gauge orbit once. A problem in the Hamiltonian formalism is that the Hamiltonian is second order in momenta, so it does not generate orbits in configuration space. On the other hand, if one goes to phase space, the Hamiltonian acts as a first-order operator and does generate orbits. Thus, from the phase space point of view, the Hamiltonian would seem

to be on an equal footing with the spatial momenta, and not singled out for special treatment. This seems to be the point of view of Ref. 38. However, we would like to offer the objection that, unlike the other gauge generators, the Hamiltonian does not simply fiber the configuration space: the Hamiltonian flow in general has a nontrivial structure, with different kinds of motion in different parts of phase space. We conjecture that it is this property, rather than the (possibly representation-dependent) second-order form of the operator, that identifies the Hamiltonian as "dynamical."

We now consider the Euclidean bounce approach. Farhi, Guth, and Guven[18] have shown that there is *no* Euclidean bounce corresponding to the nucleation of the false-vacuum bubble, if the spacetime is required to be a manifold. This is surprising, because, given our Hamiltonian formulation, there is a canonical way of constructing a Euclidean solution. In Eq. (38), we have described a family of geometries which interpolate between the two turning points. The geometries are parametrized by the bubble radius $\hat{R}$:

$$\hat{r}(\hat{R}), \quad L(r;\hat{R}), \quad R(r;\hat{R}) . \tag{57}$$

Introduce a parameter τ, which will become Euclidean time, and choose any function $\hat{R}(\tau)$ which increases monotonically from R_1 to R_2 as τ runs from 0 to 1, with $\partial_\tau \hat{R}$ vanishing linearly at the end points. Now Eq. (57) gives the wall coordinate and the spatial components of the metric as functions on Euclidean spacetime:

$$\hat{r}(\tau), \quad L(r,\tau), \quad R(r,\tau) . \tag{58}$$

The rest of the geometry, namely the metric components N^τ and N^r, is obtained by solving the relation between momenta (known from the solution of the constraints) and the time derivatives of the spatial metric [from Eq. (58)]:

$$\begin{aligned}
\partial_\tau R &= -GN^\tau i\pi_L R^{-1} + N^r R' , \\
\partial_\tau L &= -GN^\tau i\pi_R R^{-1} + GLN^\tau i\pi_L R^{-2} + (N^r L)' , \\
\partial_\tau \hat{r} &= -N^r + \frac{N^\tau i\hat{p}}{\sqrt{-L^2\hat{p}^2 + L^4\mu^2 R^4}} .
\end{aligned} \tag{59}$$

There are similar equations for the $\partial_\tau \pi_L$, $\partial_\tau \pi_R$, and $\partial_\tau \hat{p}$, but these are automatically consistent with Eqs. (59) due to the constraints.[39] The Euclidean Einstein equations are just the vanishing of the Hamiltonian and momentum densities, which hold by construction.

How is this consistent with the result in Ref. 18? It is shown in that paper that a bounce solution *is* possible, if a certain pathology is allowed. Namely, the bounce is double valued: in the exterior region $r > \hat{r}$, the mapping of the bounce spacetime into static Schwarzschild spacetime is partly two-to-one. However, we prefer an alternative description: one can unfold the bounce spacetime by a one-to-two mapping. The resulting spacetime is single-valued but still has a pathology: the vierbein is degenerate along the fold, and its determinant changes sign from one side to the other.

Returning to our canonical construction of the bounce solution, there is indeed no guarantee that the vierbein we construct is nondegenerate. The determinant of the vierbein is $N^\tau L R^2$, so the issue is the sign of the Euclidean lapse N^τ. Examination of Fig. 15 of Ref. 18 shows that the fold runs from the initial surface $\tau=0$ to the final surface $\tau=1$ along a curve $r_f(\tau)$ which lies in outside the wall, $r_f(\tau) > \hat{r}(\tau)$. In the Appendix we show that this same behavior holds for the bounce we derive from Eq. (59): the Euclidean lapse changes sign between $r=\hat{r}$ and $r \to \infty$.

In Ref. 18, a plausible prescription was made for the action of the multivalued bounce. The result agrees precisely with the WKB amplitude (50).

How are we to interpret this result? From the Euclidean point of view, it is not clear whether we should include such degenerate geometries. We might even suppose that there are two theories of gravity, one which allows only nondegenerate metrics and one which includes all metrics. However, the Hamiltonian approach gives an unambiguous answer. We have simply integrated the constraints, and have obtained a definite value for the amplitude to tunnel between the saddle points. No barrier or other ambiguity is encountered along the path of tunneling, and if the parameters describing the bubble are small compared to the Planck energy then all curvatures are also small and so semiclassical Einstein gravity is presumably valid. Thus, such degenerate bounce solutions must be admitted. The Euclidean lapse, with its usual behavior, plays no role in the Hamiltonian treatment. It is an auxiliary quantity, derived in order to give a Euclidean description of the process.

It has also been argued from a very different point of view that degenerate geometries should be allowed in quantum gravity.[40] Our result is further evidence for this. We should note, however, that the discussions in Ref. 40 were for Minkowski geometry. Further, the connection between the Euclidean bounce formalism for tunneling, and the more general Minkowski or Euclidean path-integral representations of transition amplitudes and Green's functions, seems to be understood only rather poorly and indirectly, even by the experts. The general significance of our result is therefore unclear.

Euclidean solutions which contained false-vacuum regions were also considered in Ref. 21. However, these are closed spacetimes, without initial and final hypersurfaces. Their interpretation is therefore unclear, but it does not seem to correspond to the process that we have considered.

We should point out the close similarity between the free lunch process (which can repeat within each bubble of true vacuum) and the self-reproducing universe of Linde.[22] He has considered extensively the analog of false-vacuum nucleation, but in a chaotic-inflationary potential. That is, a quantum fluctuation may produce a large potential-energy density in a region of spacetime, which then inflates before rolling down the potential. We have considered an old-inflationary potential—not because of a particular interest in this potential, but because the thin-walled spherical bubble is very simple and allows a fairly precise calculation. It seems likely that in any potential which allows inflation, a false-vacuum region can be produced by quantum fluctuation.

VII. APPLICATION: TOPOLOGY CHANGE

The evolution of the false-vacuum bubble from the turning geometry of Fig. 2(b) is quite interesting.[8–12] The bubble grows and the Schwarzschild wormhole collapses, leading to the spatial geometry shown in Fig. 4(a). The universe has two causally disconnected pieces. One is a closed space with the false-vacuum bubble and a true-vacuum region containing a black hole. The other is an infinite universe in the true-vacuum state, also containing a black hole. The black holes are at the opposite ends of the Schwarzschild singularity. If the black holes subsequently decay completely into ordinary quanta through Hawking radiation, we reach Fig. 4(b), in which the two universes are not only causally, but also topologically, disconnected.[41]

It has been proposed in recent years that topology-changing processes (wormholes) in quantum gravity have profound effects on observable physics. But we have no theory for calculating and interpreting these effects—in fact, we cannot even answer the basic question, whether topology change occurs at all. In Sec. III we made one conjecture as to why topology change might be required. The process shown in Figs. 2(a), 2(b), 4(a), and 4(b) is perhaps a more forceful argument. We have now established that the first step, quantum nucleation, occurs. We believe our argument for this step is conclusive: as noted in the preceding section, we need apply quantum gravity only in regions where the curvature is small compared to the Planck scale. The second step is purely classical.

The controversy may lie in the third step, black-hole decay. The final stages of this process involve large curvatures, where gravity is not well understood. It is a possibility that the decay terminates with a stable Planck-sized remnant of the black hole, so the two universes remain topologically connected as in Fig. 4(a). Nevertheless, we believe that one can argue for the necessity of topology change. The stable black-hole remnant looks externally like a particle, and so by general principles one believes that it must be described by a quantum field. This has a number of consequences. One is that the remnant can be produced in other ways than black-hole decay. For example, high-energy gravitons could scatter into a remnant-antiremnant pair. Further, the remnant produced from the false-vacuum bubble can annihilate with an antiremnant, completing the process of topology change.

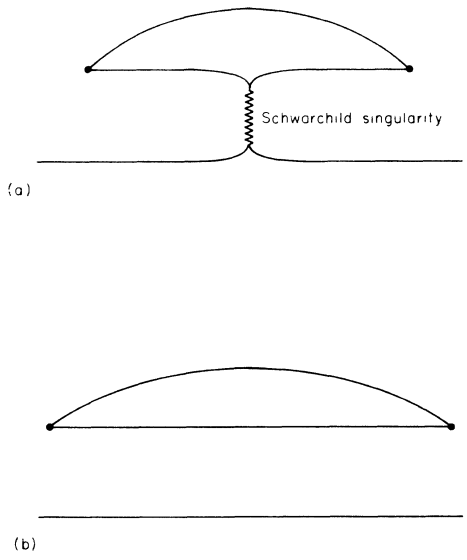

FIG. 4. (a) A spatial geometry following Fig. 2(b): the bubble has expanded and the neck has collapsed. (b) A still later geometry, after black-hole evaporation.

Even if the above arguments are correct, we have only argued that the topology of a spatial slice can change: spacetime is still simply connected. The main effects of wormholes appear only if spacetime becomes multiply connected. We have no argument that this is necessary. To conclude, we would like to emphasize that a conclusive argument that quantum gravity requires topology change would also be a starting point for the calculation and interpretation of such amplitudes.

VIII. APPLICATION: THE FREE LUNCH

We have seen that the inflating false-vacuum bubble can indeed be produced by quantum tunneling. We now ask whether this can serve the original purpose, producing matter via the free lunch process. The first issue is the rate, which is suppressed by a factor of e^{-B}, where B is given by Eq. (50):

$$B=\pi(\bar{R}-R_S)^2 l_{\text{Planck}}^{-2}\ , \tag{60}$$

with $\bar{R}$ roughly the mean of R_1 and R_2. For a bubble much larger than the Planck scale (necessary for our semiclassical calculation to be accurate) the tunneling rate is exceedingly small. Of course, the order of magnitude of B could have been written down without a detailed calculation. The main point of our work has been to show that the tunneling occurs at all—something unclear in the Euclidean and ADM approaches. The size of B may not be a problem. First, our observed universe may in fact have grown out of a Planck-sized, Planck-density bubble. This would be much harder to treat quantitatively, but there is no reason to think that the qualitative result would be different. Second, the zero-matter, zero-Λ state preceding the free lunch could have persisted for an arbitrarily long time, so any finite nucleation rate would be sufficient.

The second issue is the necessity of the seed bubble. As the mass M of the seed is taken to zero, the tunneling amplitude (50) goes to a finite limit, so the seed does not seem to be necessary. On the other hand, in this limit the turning-point geometry of Fig. 2(b) becomes degenerate. The neck shrinks to zero size, and the universe outside the neck is perfectly flat, with no evidence that nucleation has occurred. This process is indistinguishable from the birth of a false-bubble universe from nothing: the latter process and the production via nucleation must be treated in a unified way.

We turn now to our pet $\Lambda=0$ theory, the Rubakov/googolplexus.[1–3] The issue is to extend the theory from the homogeneous universes studied in Refs.

1 and 2 to universes which are inhomogeneous, but for simplicity spherically symmetric. One then asks whether the probability distribution for Λ in universes which contain an inflating false-vacuum bubble has a strong peak at zero (as it does in empty universes, but not in homogeneous warm universes). The idea of a "hot spot" in an otherwise empty universe was also raised by Rubakov.[42] Cline[3] has also suggested an inhomogeneous Rubakov/googolplexus model, and argues that a $\Lambda=0$ peak is consistent with the existence of local hot spots.

We have not yet generalized the Rubakov/googolplexus to universes containing false-vacuum bubbles; we need to extend the formalism to include creation and destruction of zero-size bubbles, and also pair production of finite-sized concentric bubbles. However, already for spherically symmetric empty universes we will encounter a potentially severe problem.

Consider a universe with the topology of a sphere,

$$0\le r\le\pi,\quad R(0)=R(\pi)=0\ . \tag{61}$$

With cosmological constant Λ and no matter, the Hamiltonian-Jacobi equations integrate readily, as in Sec. III. In the forbidden region, $R'^2/L^2<1-\Lambda R^2/3$, the wave function is

$$\Psi^{F\eta'}=\exp\frac{\eta'}{G\hbar}\int_0^\pi dr\,[\,RL\sqrt{1-\Lambda R^2/3-R'^2/L^2}\,-RR'\arccos(R'/L\sqrt{1-\Lambda R^2/3})]\ . \tag{62}$$

For spatial geometry a three-sphere of radius a,

$$L(r)=a,\quad R(r)=a\sin r\ , \tag{63}$$

the forbidden region is[43]

$$a<R_T=\sqrt{3/\Lambda} \tag{64}$$

and the wave function reduces to

$$\Psi^{F\eta'}=\exp\left[\frac{3\pi\eta'}{2\Lambda G\hbar}[1-(1-\Lambda_I a^2/3)^{3/2}]\right]\ . \tag{65}$$

The wave function Ψ^{F-}, which falls with a, has been interpreted[44] as describing tunneling from nothing, $a=0$, to a de Sitter universe in the allowed region $a>R_T$. On the other hand, generic boundary conditions at $a=0$ lead to a linear combination of Ψ^{F+} and Ψ^{F-}. At the turning point $a=R_T$, the growing wave function Ψ^{F+} dominates, and the magnitude in the classical region is

$$\exp\left[\frac{3\pi}{2\Lambda G\hbar}\right]\ . \tag{66}$$

This is the Hartle-Hawking wave function; that is, this is the wave function obtained from the no-boundary assumption plus contour prescription of Ref. 45. If some mechanism (wormholes, antisymmetric tensor field, etc.) turns Λ into a dynamical variable, then the amplitude (66) implies that the probability is concentrated entirely at $\Lambda\to0^+$. This is the idea of Hawking.[4] In third-quantized gravity, the setting for the Rubakov/googolplexus theory, the object Ψ, which we have referred to as a wave function, becomes an expectation value

$$\Psi\to\langle U|\hat{\Psi}|U\rangle\ , \tag{67}$$

where $|U\rangle$ is the third-quantized wave function and $\hat{\Psi}$ is the universe field. In spite of the extreme change of formalism, the final probability distribution is much the same as in the second-quantized theory, and for our present purposes it will be sufficient to regard Ψ as a wave function.

Now consider the amplitude for the spatial geometry shown in Fig. 5, two spheres of radius $a=R_T$ joined by a small neck:

$$L(r)=2R_T,\quad R(r)=R_T|\sin2r|+\delta R(r)\ . \tag{68}$$

Here $\delta R(r)$ is some function of order $R_{\rm neck}\ll R_T$, that smooths out the geometry near the neck at $r=\pi/2$. The neck makes only a small contribution $-\Delta\sim-R_{\rm neck}^2$ to the integral in the wave function (62). The total amplitude is

$$\exp\left[2\frac{3\pi}{2\Lambda G\hbar}-\frac{\Delta}{G\hbar}\right]\ . \tag{69}$$

As $\Lambda\to0$, this configuration seems to be much more likely than the single large sphere. We should be a little careful, however, because of the uncertainty (expressed in Sec. III) about interpreting the wave function in the forbidden region. The geometry (68) is *almost* classically allowed, but the momenta near the neck are Euclidean. This is easily remedied if there is any sort of matter in the theory. By the gravitational Gauss's law (12), adding a small amount of matter near the ends $r=0,\pi$ allows $\mathcal{M}(r)$ to vanish at 0 and π (required because these are smooth

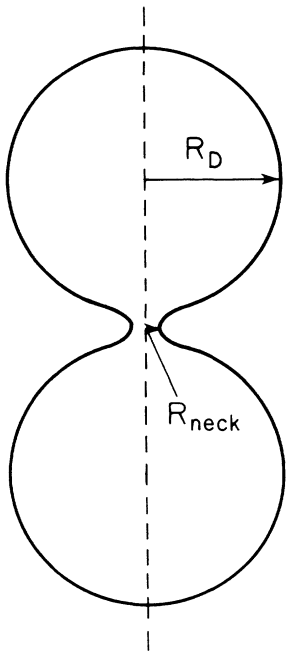

FIG. 5. Two de Sitter universes, at the turning radius, joined by a Schwarzschild wormhole.

points), and still to take a nonzero value $M_{\rm neck}$ at the neck. There is then a turning geometry with the neck a Schwarzschild wormhole of radius $2GM_{\rm neck}$, corresponding to two de Sitter spaces joined by a Schwarzschild geometry. In the Hartle-Hawking wave function this is far more likely than the single de Sitter space. In the Rubakov/googolplexus, the corresponding statement is that there are far more universes of this type than of the single de Sitter type.

Similarly, the amplitude for k spheres joined by small necks is

$$\exp\left[k\frac{3\pi}{2\Lambda G\hbar}-(k-1)\frac{\Delta}{G\hbar}\right] . \tag{70}$$

The sum over k diverges, indicating that the distribution is dominated (in this spherically symmetric ansatz) by an infinite chain of spheres and necks. This is not fatal in itself, because an observer in one universe sees only his local de Sitter space, plus two black holes. Now let us relax the spherical symmetry, and allow Schwarzschild wormholes to be inserted anywhere. The divergence in the sum over k makes the distribution difficult to define. Let us cut the sum off at some large value of k (the Rubakov/googolplexus would suggest the value $k_{\rm max}\sim e^{3\pi/\Lambda}$). Now consider a point p in one of the de Sitter spaces, and compare the amplitude for the geometry at p to be smooth with that to find a Schwarzschild wormhole end (black hole) at p. In the latter case, there is a suppression factor $e^{-\Delta}$, but a combinatoric factor $O(k_{\rm max})$ from the possible locations of the other end of the wormhole. As $k_{\rm max}\to\infty$ (or even $\to e^{3\pi/\Lambda}$) the combinatoric factor overwhelms the suppression. We conclude that the Hartle-Hawking wave function predicts that black holes are dense in spacetime. This is the best case: it could be that it is too divergent to make sense at all.

This is very similar to the large wormhole problem,[24] except that we are always talking about the geometry of space, not spacetime. It seems very probable that any assumptions about quantum gravity which lead to the famous $e^{3\pi/2\Lambda}$ will give rise to such pathologies.

Those familiar with the Euclidean approach to the Hartle-Hawking wave function will be surprised by our conclusion, because the single de Sitter sphere is believed to be the gravitational instanton of least action. However, we have argued in Sec. VI that consistency with the Hamiltonian approach requires the inclusion in the Euclidean path integral of saddle points with degenerate metric. We have also in that section shown how the Euclidean solution can be constructed from the Hamiltonian description of the tunneling.

IX. CONCLUSIONS

Using Dirac quantization, we have shown that the inflating false-vacuum bubble can be produced by quantum tunneling. We have seen, in Sec. VI, why the ADM and Euclidean bounce methods give ambiguous answers. In the latter case, consistency with the Hamiltonian requires the inclusion of Euclidean spacetimes with indefinite metric. Along the way we have raised several questions about the formal structure of quantum gravity, including the significance of the amplitude to find a forbidden geometry (Sec. III) and the sense in which the Hamiltonian constraint is special (Sec. VI). We have proposed two tentative arguments for the necessity of topology change (Secs. III and VII). Applying our results to quantum cosmology, we find a possibly fatal divergence in the Hartle-Hawking wave function, and a severe problem for the Hawking and Rubakov/googolplex theories of the cosmological constant. We believe that all of these points merit further development.

ACKNOWLEDGMENTS

We would like to thank E. Farhi and A. Guth for the seminars which inspired our interest in this problem, and for discussions of their work. We would also like to thank many of the participants of the Aspen Center for Physics for their comments, in particular S. Coleman, G. Horowitz, A.Strominger, L. Susskind, and W. Unruh. This research was supported in part by the Robert A. Welch Foundation and NSF Grant No. PHY8605978. J.P. was supported in part by the A. P. Sloan Foundation.

APPENDIX

In this appendix, we show that the Euclidean solution whose construction was described in Sec. VI must be degenerate in places. To be precise, we will show that the Euclidean lapse N^τ, which determines the sign of the determinant of the vierbein, is positive on the world line of the bubble but negative in some part of the exterior of the bubble (or vice versa).

First, recall some features of the geometry, Eqs. (37) and (38). The radial coordinate is defined by $L(r)=1$, so that r is equal to *proper radius*, the geodesic distance from $r=0$. The momentum $\hat{p}$ vanishes, while $i\pi_L(r)$ is negative definite (for Ψ^{F^-}) and falls rapidly to zero at infinity. Also, $\hat{R}$ increases monotonically with τ.

In Eq. (59), combining the results for $\partial_\tau\hat{r}$ and $\partial_\tau R(\hat{r}+\epsilon)$ implies that

$$\hat{N}^\tau=-\hat{R}\,\partial_\tau\hat{R}/Gi\hat{\pi}_L . \tag{A1}$$

The right-hand side is positive definite. Incidentally, it is not hard to show from Eq. (59) that N^τ and N^r are continuous at the kink.

Now consider a spherical shell of transverse radius $R_0\gg R_2$. The proper radius of the shell is $r_0(\tau)$, defined by $R[r_0(\tau),\tau]=R_0$. At R_0, the geometry is essentially flat three-space, because of the rapid falloff of π_L. Therefore, $R(r,\tau)\to r+\zeta(\tau)$ for some function $\zeta(\tau)$. Thus, $r_0(\tau)=R_0-\zeta(\tau)$. From the $\partial_\tau R$ equation,

$$-N^r(r_0,\tau)=-\partial_\tau\zeta=\partial_\tau r_0 . \tag{A2}$$

In other words, $-N^r(r_0,\tau)$ is the τ derivative of the proper radius of the R_0 shell. On the other hand, it follows directly from the $\partial_\tau\hat{r}$ equation that $-\hat{N}^r(\tau)$ is the τ derivative of the proper radius of the bubble.

Finally, integrate the $\partial_\tau L$ equation, at fixed τ, from $\hat{r}(\tau)$ to $r_0(\tau)$. Using the relation $\pi_R=-b\pi_L/R$ from Eq. (38) gives

$$-N^r(r_0,\tau)+\hat{N}^r(\tau) = \int_{\hat{r}}^{r_0} dr[(b+1)Gi\pi_L(r,\tau)/R^2(r,\tau)]N^\tau(r,\tau) . \quad \text{(A3)}$$

The left-hand side is, by the preceding paragraph, the time derivative of the proper distance from the bubble to the R_0 shell. It is obvious by inspection of Fig. 2 that this proper distance undergoes a net increase, precisely because of the bending in of the neck (note that proper distance is measured along the curves in Fig. 2). Equivalently, the increase is equal to the proper distance from point 1 to point 2 in Fig. 3. Thus, the left-hand side is positive for some, if not all, τ. On the other hand, the quantity in square brackets on the right-hand side is negative definite. Therefore the lapse $N^\tau(r,\tau)$ must be negative in part of the exterior. Q.E.D.

[1]V. A. Rubakov, Phys. Lett. B **214**, 503 (1988).

[2]W. Fischler, I. Klebanov, J. Polchinski, and L. Susskind, Nucl. Phys. **B327**, 157 (1989).

[3]J. Cline, Ohio State University Report No. DOE/ER/01545-432, 1989 (unpublished).

[4]S. W. Hawking, Phys. Lett. **134B**, 403 (1984).

[5]L. Abbott, Phys. Lett. **150B**, 427 (1985).

[6]J. D. Brown and C. Teitelboim, Nucl. Phys. **B297**, 787 (1987).

[7]The solution proposed by S. Coleman, Nucl. Phys. **B310**, 643 (1988), may not have this property because the probability distribution for couplings in our warm universe is determined by dynamics in other, cold universes. Whether Coleman's idea is consistent with a warm universe depends on further details which are not now understood. Some discussion of this appears in I. Klebanov, L. Susskind, and T. Banks, Nucl. Phys. **B317**, 665 (1989).

[8]K. Sato, M. Sasaki, H. Kodama, and K. Maeda, Prog. Theor. Phys. **65**, 1443 (1981); H. Kodama, M. Sasaki, K. Sato, and K. Maeda, *ibid.* **66**, 2052 (1981); K. Sato, *ibid.* **66**, 2287 (1981); H. Kodama, M. Sasaki, and K. Sato, *ibid.* **68**, 1979 (1982); K. Maeda, K. Sato, M. Sasaki, and H. Kodama, Phys. Lett. **108B**, 98 (1982); K. Sato, H. Kodama, M. Sasaki, and K. Maeda, *ibid.* **108B**, 103 (1982).

[9]K. Lake, Phys. Rev. D **19**, 2847 (1979); K. Lake and R. Wevrick, Can. J. Phys. **64**, 165 (1986).

[10]V. A. Berezin, V. A. Kuzmin, and I. I. Tkachev, Phys. Lett. **120B**, 91 (1983); Phys. Rev. D **36**, 2919 (1987); in *Quantum Gravity,* proceedings of 3rd Seminar on Quantum Gravity, Moscow, USSR, 1984, edited by M. A. Markov, V. A. Berezin, and V. P. Frolov (World Scientific, Singapore, 1985), p. 605.

[11]A. Aurilia, G. Denardo, F. Legovini, and E. Spallucci, Phys. Lett. **147B**, 258 (1984); Nucl. Phys. **B252**, 523 (1985); A. Aurilia, M. Palmer, and E. Spallucci, Phys. Rev. D **40**, 2511 (1989).

[12]S. K. Blau, E. I. Guendelman, and A. H. Guth, Phys. Rev. D **35**, 1747 (1987).

[13]S. Coleman, Phys. Rev. D **15**, 2929 (1977).

[14]S. Coleman and F. DeLucchia, Phys. Rev. D **21**, 3305 (1980).

[15]E. Farhi and A. H. Guth, Phys. Lett. B **183**, 149 (1987).

[16]A. H. Guth, presented at seminar, University of Texas, 1988 (unpublished).

[17]W. Fischler, D. Morgan, and J. Polchinski, Phys. Rev. D **41**, 2638 (1990). We should also note the following misprints in this earlier paper: the expression for $\mathcal{M}'$ above Eq. (6) should be divided by L, and the sign of the Λ term in Eq. (6) should be changed.

[18]E. Farhi, A. H. Guth, and J. Guven, Nucl. Phys. **B339**, 417 (1990).

[19]S. W. Hawking, Phys. Lett. B **195**, 337 (1987); S. B. Giddings and A. Strominger, Nucl. Phys. **B306**, 890 (1988).

[20]V. A. Berezin, V. A. Kuzmin, and I. I. Tkachev, Phys. Lett. B **207**, 397 (1988).

[21]V. A. Berezin, N. G. Kozimirov, V. A. Kuzmin, and I. I. Tkachev, Phys. Lett. B **212**, 415 (1988).

[22]A. D. Linde, *Particle Physics and Inflationary Cosmology* (Gordon and Breach, New York, 1989).

[23]A. S. Goncharov, A. D. Linde, and V. F. Mukhanov, Int. J. Mod. Phys. A **2**, 561 (1987).

[24]W. Fischler and L. Susskind, Phys. Lett. B **217**, 48 (1989); J. Polchinski, Nucl. Phys. **B325**, 619 (1989).

[25]P. A. M. Dirac, Proc. R. Soc. London **A246**, 333 (1958).

[26]R. Arnowitt, S. Deser, and C. W. Misner, in *Gravitation: An Introduction to Current Research,* edited by L. Witten (Wiley, New York, 1962).

[27]It would be an interesting exercise, which we have not seen done, to work out the semiclassical limit of BRST quantization explicitly, and show that it is equivalent to imposing all of the constraints in a naive way.

[28]B. K. Berger, D. M. Chitre, V. E. Moncrief, and Y. Nutku, Phys. Rev. D **5**, 2467 (1972).

[29]W. G. Unruh, Phys. Rev. D **14**, 870 (1976).

[30]P. Thomi, B. Isaak, and P. Hajicek, Phys. Rev. D **30**, 1168 (1984).

[31]The constraints might seem to allow η in π_L to have different signs at different points, and π_R to have δ functions, but one can check that this is inconsistent with the WKB approximation.

[32]The analogy with the string also suggests an answer to our question about the observability of the wave function, and about the observables in quantum gravity more generally.

[33]V. A. Rubakov, Nucl. Phys. **B203**, 311 (1982); C. G. Callan, Phys. Rev. D **25**, 2141 (1982).

[34]Another way to characterize the allowed and forbidden regions is as follows. The vectors $\mathbf{V}(\hat{r}+\epsilon)$, $\mathbf{V}(\hat{r}-\epsilon)$, and $\mathbf{V}_M$ have the respective lengths squared $1-(\Lambda_I\hat{R}^2/3)$, $1-(2GM/\hat{R})$, $\mu^2L^2\hat{R}^4$, and they are further related by Eq. (31). Therefore, if the three lengths satisfy the Lorentzian triangle inequality (one length *greater than* the sum of the other two, or one or two lengths squared negative), there will be a solution with real momenta and $\hat{R}$ is in the allowed region. If the three lengths satisfy the usual Euclidean triangle inequality, the momenta are imaginary and $\hat{R}$ is in the forbidden region.

[35]Our confusion about the meaning of the wave function, expressed in Sec. III, should not be a problem here, since the tunneling can be observed in the late-time classical region.

[36]We should point out that in this case the wave function corresponding to bubble nucleation is Ψ^+, while in the false-vacuum bubble case it was Ψ^-. We do not understand the significance of this, but it depends in part on the choice of O(1,1) frame at the wall. In the Euclidean approach of Ref. 18, it was also found necessary to choose the sign of the action by hand.

[37]This slice does not satisfy the discontinuity relations (26): the spatial geometry at the wall is more kinked than necessary. This is no problem. We can consider such a geometry as a limit of geometries in which the kink is smoothed out.

[38]R. Woodard, Brown Report No. HET-728, 1989 (unpublished).

[39]If Eqs. (59) are degenerate, for example, when $\pi_R = \pi_L = 0$, the time derivatives of the momenta determine the lapse and shift.

[40]A. Ashtekar, Phys. Rev. Lett. **57**, 2244 (1986); E. Witten, Nucl. Phys. **B311**, 46 (1988–89).

[41]In Ref. 23, it is argued that this same kind of process occurs in a chaotic-inflationary potential.

[42]V. A. Rubakov, presented at the Fermilab Wormshop, 1989 (unpublished).

[43]The cosmological constant is assumed positive. For negative Λ, there is no allowed region.

[44]A. D. Linde, Zh. Eksp. Teor. Fiz. **87**, 369 (1984) [Sov. Phys. JETP **60**, 211 (1984)]; Lett. Nuovo Cimento **39**, 401 (1984); Ya. B. Zeldovich and A. A. Starobinsky, Pis'ma Astron. Zh. **10**, 323 (1984) [Sov. Astron. Lett. **10**, 135 (1984)]; V. A. Rubakov, Phys. Lett. **148B**, 280 (1984); A. Vilenkin, Phys. Rev. D **30**, 549 (1984).

[45]J. B. Hartle and S. W. Hawking, Phys. Rev. D **28**, 2960 (1983). This Hamiltonian interpretation was given by A. Strominger, Nucl. Phys. **B319**, 722 (1989).